

Overview of Recent Experimental Electroweak Probes Results

Austin Baty^{a,*}

*^aDepartment of Physics and Astronomy, Rice University,
6100 Main St, Houston, TX, 77005, USA*

E-mail: abaty@rice.edu

Electroweak probes have no color charge and therefore do not interact via the strong force. Somewhat paradoxically, this makes them an excellent probe of the strongly-coupled quark-gluon plasma created in high energy heavy ion collisions. Recent experimental results are discussed for three classes of electroweak probe. The first class concerns the usage of heavy bosons for constraining the initial stages of a heavy ion collisions. The second class of probes involves the back-to-back leptons produced in electromagnetic processes which are typically thought of in the context of ultraperipheral collisions. The final class of probes discussed involves direct photons and low mass dilepton pairs, which can be used to constrain the temperature of the QGP fireball and learn about the evolution of the QGP medium. Finally, some recent related measurements which might have implications for future searches for beyond the Standard Model physics are addressed. In all cases, significant recent progress has been made on the experimental front, and exciting new opportunities for future measurements still exist.

*HardProbes2023
26-31 March 2023
Aschaffenburg, Germany*

*Speaker

1. Introduction

Although it might seem contradictory, some of the most powerful tools for studying the properties of the quark-gluon plasma (QGP), whose dynamics are predominantly dictated by Quantum Chromodynamics (QCD), are electroweak probes which have no intrinsic color charge. Heavy bosons, such as the W and Z , allow experimental access to the very initial stages of a heavy ion collision which creates the QGP, and therefore provide strong constraints on parton distribution functions (pdfs) and initial collision geometry. A less canonical electroweak probe — back-to-back lepton pairs created in the $\gamma\gamma \rightarrow \ell^-\ell^+$ process — may also be able to provide useful information about the nature of heavy ion collisions, but the experimental understanding of this process as a probe for hadronic heavy ion collisions is still in a nascent stage. Finally, lower mass and transverse momentum (p_T) photons and dilepton pairs can give access to the evolution of the QGP fireball, and provide constraints on the effective temperature of the medium. Recent developments for each of these three classes of electroweak probe are discussed in more detail in the subsequent sections, and an exciting related measurement with implications for beyond the Standard Model (BSM) physics is also discussed.

2. Tests of the initial state with heavy electroweak bosons

Heavy electroweak bosons have lifetimes that are on the same order as that of the formation time of the QGP, and have significant branching ratios to decay channels that involve purely leptonic states. Because the resulting high- p_T leptons barely interact with the medium and are relatively straightforward to detect experimentally, they allow access to the kinematic information of the

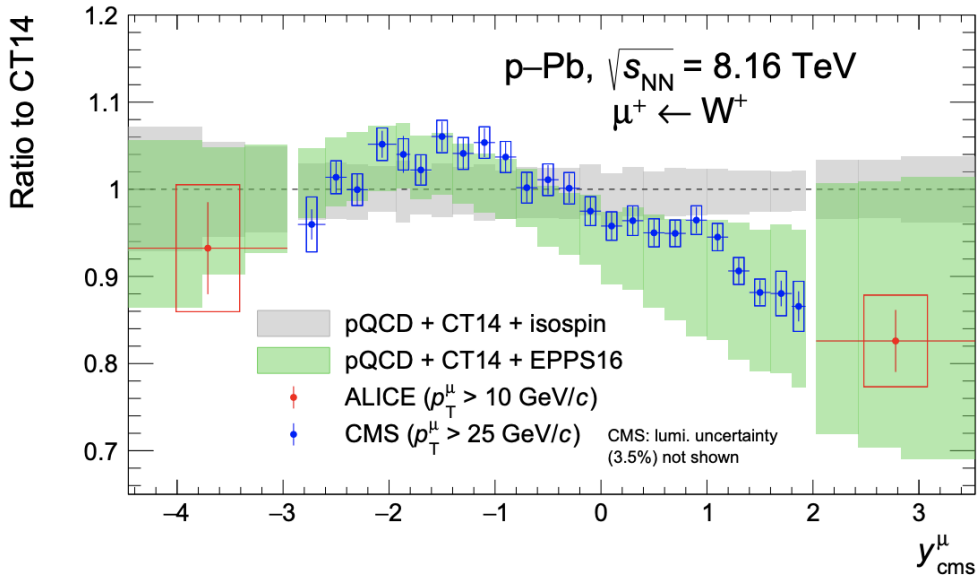


Figure 1: A ratio of the yields of W^+ bosons in 8.16 TeV pPb collisions to a pQCD prediction using various n(PDFs). New data from the ALICE Collaboration are shown in the far forward and backward region [1]. Data from the CMS Collaboration are shown in the midrapidity region [2]. Figure reproduced from Ref. [1].

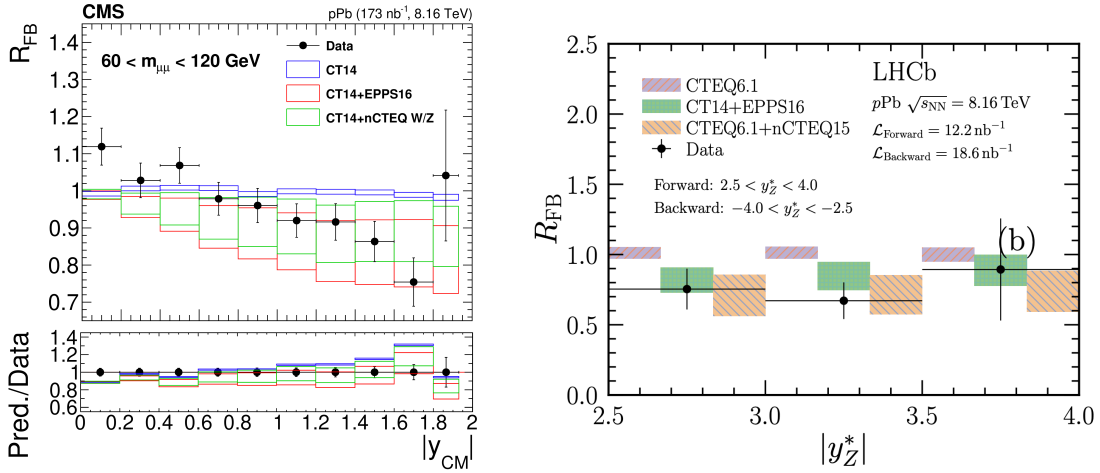


Figure 2: Forward-backwards ratios for Z/γ^* boson production in 8.16 TeV pPb collisions from the CMS [6] (left) and LHCb [7] (right) Collaborations. The CMS data covers the rapidity region $0 < |y_{CM}| < 2$, while the LHC data extends to $2.5 < |y_{CM}| < 4$. Different (n)PDF sets are also shown.

original boson with very high fidelity. All of these considerations result in heavy electroweak bosons being powerful and clean probes of the initial state of a heavy ion collision which can test models of parton distribution functions, as well as models of the distributions of nucleons within a nucleus.

Figure 1 shows a compilation of results from the ALICE [1] and CMS Collaborations [2] for W^+ boson production in proton-lead collisions at $\sqrt{s_{NN}} = 8.16$ TeV. To better show the effects of nPDF effects, the data are divided by a pQCD model that uses the CT14[3] free proton pdf. A clear indication of anti-shadowing (shadowing) can be seen in the blue CMS data for the rapidity region of $-3 < y < -1$ ($0 < y < 2$). The newer red ALICE data extends these measurements to a more forward region, where it supports a strong shadowing effect, and also towards the backwards region, where a potential hint of the EMC effect can be seen, although there are still significant measurement uncertainties. The data agree well with the green band showing the effect of the EPPS16 nPDF set [4], and it should be noted that the updated EPPS21 nPDF set [5] has included the CMS data in their model to improve its precision.

Figure 2 shows measurements by the CMS [6] and LHCb Collaborations [7] of Z/γ^* boson production in 8.16 TeV pPb collisions. In particular, the forward-backward ratio is shown, as this observable allows for cancellation of uncertainties and subsequently a greater sensitivity to nPDF effects. It should also be noted that by combining the unique information provided by these detectors, almost the full rapidity range $|y_{CM}| < 4$ can be probed. Comparisons are shown versus models using the free proton pdf, as well as including the effects of nPDFs as modeled by EPPS16 [4] and nCTEQ15 [8]. The data agree with the models using nPDFs nicely and in some cases have smaller uncertainties, which indicate that nPDFs can be further constrained by these data. The data once again support strong nuclear shadowing in the forward rapidity region, combined with an anti-shadowing effect in the backward region.

The yields of electroweak bosons in lead-lead collisions can also be used to constrain the initial state by testing the frequently used Glauber model [9], which models the initial geometry of heavy

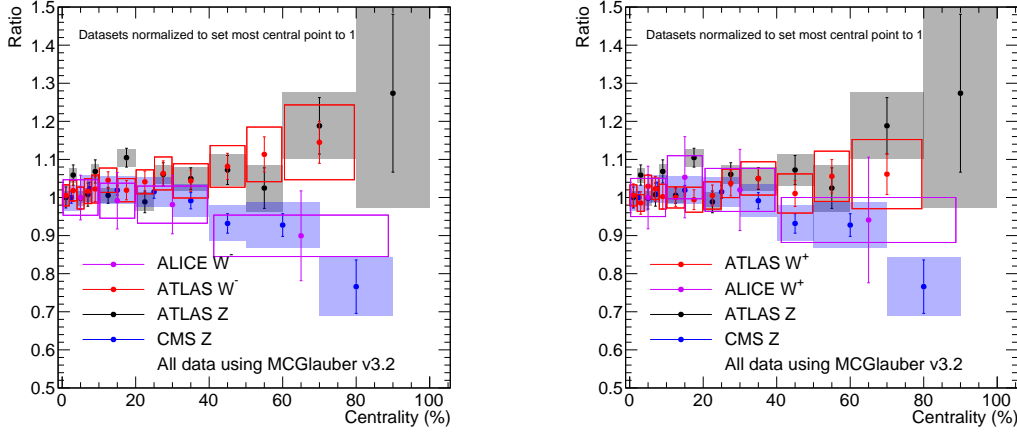


Figure 3: A comparison between results from the ALICE [1], ATLAS [10], and CMS [11] Collaborations for electroweak boson production in lead-lead collisions. The data have been normalized such that the most central data point is equal to unity to allow a comparison of the shape of the distribution. The left panel shows results for W^- and Z bosons, while the right panel shows results for W^+ and Z bosons.

ion collisions and is used to calculate the average number of colliding nucleons (N_{col}) at a given centrality. Typically, it is expected that the yields of massive electroweak bosons, when scaled by N_{col} (i.e., the numerator of a nuclear modification factor R_{AA}) should be flat as a function of centrality. Although this appears to be approximately the case for the 0–50% centrality range, recent measurements for peripheral events have challenged this thought.

Figure 3 summarizes these measurements from the ALICE [1], ATLAS [10], and CMS [11] Collaborations for W and Z bosons in lead-lead collisions at 5.02 TeV. To make a comparison of the shapes of these distributions rather than their overall normalization and remove isospin effects (which cause the yields of W^+ and W^- bosons to differ significantly), the datasets have been normalized to set the most central data point to unity. Additionally, ATLAS reported their data using two different versions of the Glauber model, MCGlauber v2.4 versus MCGlauber v3.2 [12]. Here we take the v3.2 data to make a fair comparison to the measurements done by other collaborations. This marginally improves the agreement of the various datasets with each other. In general the ATLAS data exhibits a weak upward trend as centrality increases for both the Z and W channels, which was thought to potentially be caused by shadowing of the total nucleon-nucleon cross section [13]. Conversely, the CMS Z boson data shows a pronounced downward trend which seems to agree with the predictions of the HG-PYTHIA [14] model incorporating selection and centrality calibration effects. The ALICE W data lies between the ATLAS and CMS data, and is consistent with both the HG-PYTHIA prediction and the assumption of a perfectly flat centrality dependence, but does not support a shadowed nucleon-nucleon cross section. Thus, there appears to still be some tension in the various measurements and their physics interpretations, although it should be kept in mind that there are still significant uncertainties. New data from the LHC Run 3 can help resolve this discrepancy, but experiments should be mindful of the difficulties associated with the centrality

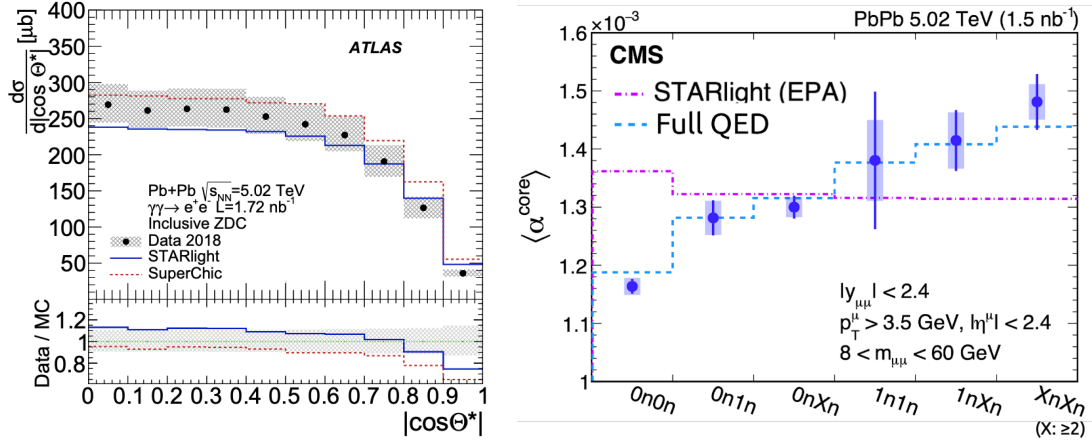


Figure 4: (Left) A measurement of the differential cross section of dielectrons produced in ultraperipheral PbPb collisions as a function of $|\cos \Theta^*|$, as measured by the ATLAS Collaboration [16]. (Right) A CMS measurement of the extracted average of the “core” part of the acoplanarity distribution of dimuons produced in ultraperipheral PbPb collisions. The results are displayed for various forward neutron classes [17].

calibrations and the ‘anchor points’ used in these peripheral regions [15].

3. The $\gamma\gamma \rightarrow \ell^+\ell^-$ process — a tool to understand the QGP

Heavy ions have very strong electric fields surrounding them, which can be treated as a flux of photons using the equivalent photon approximation. When two ions interact but have an impact parameter greater than twice the nuclear radius, the collision is said to be an ultraperipheral collision (UPC). UPCs can generate exceptionally clean final states containing two nearly back-to-back leptons in the process $\gamma\gamma \rightarrow \ell^-\ell^+$, allowing precise tests of Quantum Electrodynamics (QED) processes. Rather recently, it has been observed that the same clean electromagnetic processes that occur in UPCs can also occur even when the two nuclei undergo a hadronic collision which is not a UPC. In principle, it is then possible to use UPCs to study the details of QED dilepton production, and then explore if the QGP medium created in hadronic collisions further modifies the final state of this system. In this way, electromagnetic back-to-back lepton production can be considered one of the newest tools available for they study of the production of the QGP.

Before examining the properties of the QGP, the precise details of the signal electromagnetic process $\gamma\gamma \rightarrow \ell^-\ell^+$ must be understood. Figure 4 shows some key recent measurements promoting this goal. The left panel shows a measurement by the ATLAS Collaboration of $|\cos \Theta^*| = |\tanh \Delta\eta_{ee}/2|$ for the UPC process $\gamma\gamma \rightarrow e^-e^+$ in 5.02 TeV PbPb collisions [16], where $\Delta\eta_{ee}$ is the difference in pseudorapidity between the two electrons in the pair. In general, the data lies in the envelope spanned by the STARlight [18] and SuperChic [19] Monte Carlo generators. However, deviations are observed for large values of $|\cos \Theta^*|$, corresponding to the region where higher-energy initial photons are involved in the process. Thus, there is some indication of potential improper modeling of these higher-energy contributions in these models. The right panel of Fig. 4 shows a measurement of the $\gamma\gamma \rightarrow \mu^-\mu^+$ process by the CMS Collaboration for 5.02 TeV PbPb collisions [17]. Here, the acoplanarity $\alpha = 1 - |\Delta\phi_{\mu\mu}|/\pi$ distribution is measured, where $\Delta\phi_{\mu\mu}$ is the difference in azimuthal

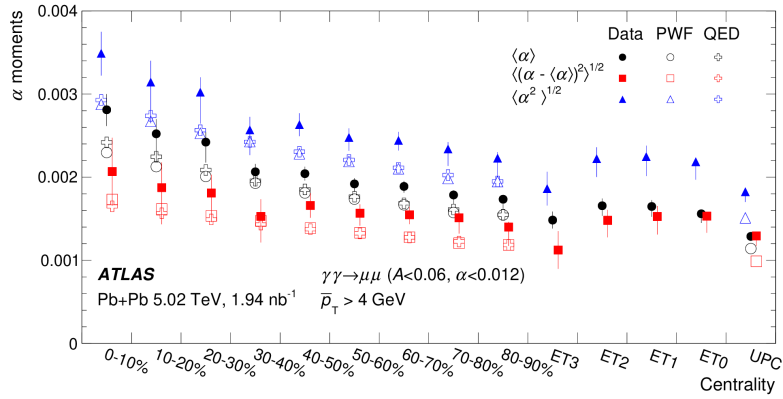


Figure 5: The ATLAS Collaboration’s measurement of the moments of the acoplanarity distribution of muon pairs produced in the electromagnetic process $\gamma\gamma \rightarrow \mu^+\mu^-$ for various event classes, ranging from central hadronic PbPb collisions to ultraperipheral collisions. Figure reproduced from Ref. [21].

angle between muons, and then the width of the ‘core’ part of the distribution is measured. This width, $\langle \alpha \rangle$ is thought to correspond with the leading-order contribution to this dimuon production process. The value $\langle \alpha \rangle$ is then plotted as a function of the number of neutrons detected in the forward region along the beam line using zero degree calorimeters. Here, the notation $AnBn$ corresponds to detecting A neutrons in one side of the detector and B neutrons in the other side. A larger amount of forward neutron production is correlated with a smaller impact parameter between the two ions (although the impact parameter is still greater than 2 times the nuclear radius), and also with a larger flux of relatively higher-energy initial state photons. The leading-order STARlight model [18] does not account of this impact-parameter dependence of the photon flux, and thus cannot capture the rising trend seen in the CMS data. However, a full QED calculation including this effect [20] is able to describe the data well. Thus, a key conclusion from these measurements is that the impact-parameter dependence of the photon flux at a given energy must be fully understood and modeled to describe even these relatively clean QED processes.

Figure 5 shows a similar measurement of the moments of the α distribution for the $\gamma\gamma \rightarrow \mu^-\mu^+$ process for 5.02 TeV PbPb collisions [21]. The measurements are displayed as a function of decreasing event activity, starting with central 0–10% hadronic collisions (where a QGP is clearly expected to be formed) all the way to UPC collisions. Thus, this measurement *leverages the unique back-to-back topology of the muons originating from this EM process to actually probe the effects of the presence of a QGP as compared to the vacuum case*. In general, a broadening of the acoplanarity is observed as event activity increases (and impact parameter decreases). This is why the understanding of the α broadening in the UPC events is so important, as a similar effect can be observed in hadronic collisions. The broadening in hadronic collisions could possibly be the result of Coulomb scattering of the decay muons off medium constituents, but it appears that QED calculations including impact parameter dependent photon flux can approximately capture the trend. These data were also used to exclude models of magnetic-field induced broadening of the dimuon pairs. This measurement clearly shows the potential of the $\gamma\gamma \rightarrow \ell^-\ell^+$ process (and the related understanding gained from UPC collisions) as a new electromagnetic probe of the QGP

common source as the fireball evolves through the phase transition, the characteristic temperature of which should be independent of the initial collision energy. The right panel of Figure 6 shows a summary from the STAR Collaboration of the effective temperature of the QGP, as measured using low-mass (LMR) and intermediate-mass (IMR) dileptons, as well as direct photons, as a function of the baryon number chemical potential, μ_B [23]. The results from direct photons tend to be larger than those for dileptons indicating that these two methods may probe slightly different times of the QGP evolution, or that other effects must be taken into account when calculating the effective temperature of the medium. Interestingly, not much data is available in the high $\mu_B \approx 1000$ MeV region, but it is expected that more data in this region will be available soon because of additional experimental efforts. For example a precise dielectron spectrum from the HADES experiment, along with known hadronic backgrounds, is shown in Fig. 7 for silver-silver collisions at $\sqrt{s_{NN}} = 2.55$ GeV. Thus, direct photons and thermal dileptons represent a powerful tool for the probing of the QCD phase diagram and the thermal properties of the QGP.

5. Exploring $\gamma\gamma \rightarrow \tau^+\tau^-$

The production of dileptons is not just useful for examination of the QGP. Recently, both the ATLAS [26] and CMS [25] Collaborations have observed the $\gamma\gamma \rightarrow \tau^+\tau^-$ process in UPC lead-lead collisions. Figure 8 shows a summary of the results, including a plot of the invariant ditau mass used by CMS to observe this process, and a figure of the anomalous magnetic moment, $a_\tau = (g - 2)/2$, where g is the gyromagnetic ratio. The value a_τ is particularly interesting because it is potentially sensitive to higher-order corrections from BSM particles if one can measure it with sufficient precision. Although the current measurements are still less precise than the current best result from e^+e^- collisions, it may be possible with LHC Run 3 and 4 data to set new constraints on BSM physics. Thus, our understanding of UPC physics may also have a direct impact on fundamental questions in high energy physics.

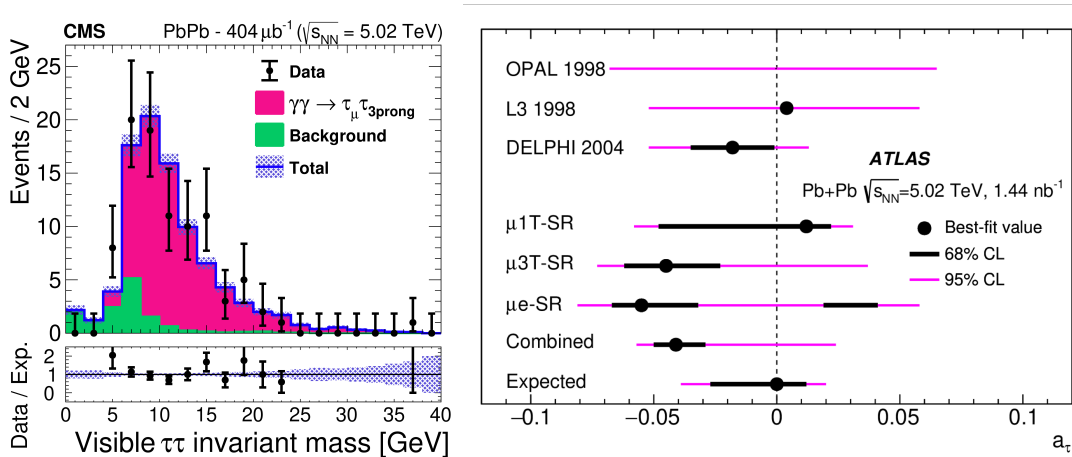


Figure 8: (Left) The ditau invariant mass for, as observed by the CMS Collaboration, that is used in the observation of the $\gamma\gamma \rightarrow \tau^+\tau^-$ process in ultraperipheral PbPb collisions [25]. (Right) The ATLAS Collaboration measured the same process simultaneously, and both experiments were able to set constraints on the τ anomalous magnetic moment, a_τ [26].

6. Summary

There has been ample progress in recent years to fully utilize the gamut of electroweak probes to characterize not only the QGP, but other fundamental scattering processes. Significant constraints have been applied on nPDF models, but some clarification is still needed when examining PbPb collisions. The improved understanding of UPC events made possible by recent measurements has allowed us to promote the electromagnetic production of back-to-back lepton pairs from photons to a probe of the medium in hadronic collisions. Finally, further constraints on the evolution and temperature of the medium have been made possible by recent measurements of direct photons and low mass dileptons, with more experimental data still to come.

References

- [1] ALICE collaboration, *W^\pm -boson production in p -Pb collisions at $\sqrt{s_{NN}} = 8.16$ TeV and PbPb collisions at $\sqrt{s_{NN}} = 5.02$ TeV*, *JHEP* **05** (2023) 036 [2204.10640].
- [2] CMS collaboration, *Study of W boson production in pPb collisions at $\sqrt{s_{NN}} = 5.02$ TeV*, *Phys. Lett. B* **750** (2015) 565 [1503.05825].
- [3] S. Dulat, T.-J. Hou, J. Gao, M. Guzzi, J. Huston, P. Nadolsky et al., *New parton distribution functions from a global analysis of quantum chromodynamics*, *Phys. Rev. D* **93** (2016) 033006 [1506.07443].
- [4] K.J. Eskola, P. Paakkinen, H. Paukkunen and C.A. Salgado, *EPPS16: Nuclear parton distributions with LHC data*, *Eur. Phys. J. C* **77** (2017) 163 [1612.05741].
- [5] K.J. Eskola, P. Paakkinen, H. Paukkunen and C.A. Salgado, *EPPS21: a global QCD analysis of nuclear PDFs*, *Eur. Phys. J. C* **82** (2022) 413 [2112.12462].
- [6] CMS collaboration, *Study of Drell-Yan dimuon production in proton-lead collisions at $\sqrt{s_{NN}} = 8.16$ TeV*, *JHEP* **05** (2021) 182 [2102.13648].
- [7] LHCb collaboration, *Measurement of the Z boson production cross-section in proton-lead collisions at $\sqrt{s_{NN}} = 8.16$ TeV*, *JHEP* **06** (2023) 022 [2205.10213].
- [8] K. Kovarik et al., *nCTEQ15 - Global analysis of nuclear parton distributions with uncertainties in the CTEQ framework*, *Phys. Rev. D* **93** (2016) 085037 [1509.00792].
- [9] M.L. Miller, K. Reygers, S.J. Sanders and P. Steinberg, *Glauber modeling in high energy nuclear collisions*, *Ann. Rev. Nucl. Part. Sci.* **57** (2007) 205 [nucl-ex/0701025].
- [10] ATLAS collaboration, *Z boson production in Pb+Pb collisions at $\sqrt{s_{NN}} = 5.02$ TeV measured by the ATLAS experiment*, *Phys. Lett. B* **802** (2020) 135262 [1910.13396].
- [11] CMS collaboration, *Constraints on the Initial State of Pb-Pb Collisions via Measurements of Z -Boson Yields and Azimuthal Anisotropy at $\sqrt{s_{NN}} = 5.02$ TeV*, *Phys. Rev. Lett.* **127** (2021) 102002 [2103.14089].

- [12] C. Loizides, *Glauber modeling of high-energy nuclear collisions at the subnucleon level*, *Phys. Rev. C* **94** (2016) 024914 [1603.07375].
- [13] K.J. Eskola, I. Helenius, M. Kuha and H. Paukkunen, *Shadowing in inelastic nucleon-nucleon cross section?*, *Phys. Rev. Lett.* **125** (2020) 212301 [2003.11856].
- [14] C. Loizides and A. Morsch, *Absence of jet quenching in peripheral nucleus–nucleus collisions*, *Phys. Lett. B* **773** (2017) 408 [1705.08856].
- [15] F. Jonas and C. Loizides, *Centrality dependence of electroweak boson production in PbPb collisions at the CERN Large Hadron Collider*, *Phys. Rev. C* **104** (2021) 044905 [2104.14903].
- [16] ATLAS collaboration, *Exclusive dielectron production in ultraperipheral Pb+Pb collisions at $\sqrt{s_{NN}} = 5.02$ TeV with ATLAS*, 2207.12781.
- [17] CMS collaboration, *Observation of Forward Neutron Multiplicity Dependence of Dimuon Acoplanarity in Ultraperipheral Pb-Pb Collisions at $\sqrt{s_{NN}}=5.02$ TeV*, *Phys. Rev. Lett.* **127** (2021) 122001 [2011.05239].
- [18] S.R. Klein, J. Nystrand, J. Seger, Y. Gorbunov and J. Butterworth, *STARlight: A Monte Carlo simulation program for ultra-peripheral collisions of relativistic ions*, *Comput. Phys. Commun.* **212** (2017) 258 [1607.03838].
- [19] L.A. Harland-Lang, V.A. Khoze and M.G. Ryskin, *Exclusive physics at the LHC with SuperChic 2*, *Eur. Phys. J. C* **76** (2016) 9 [1508.02718].
- [20] J.D. Brandenburg, W. Li, L. Ruan, Z. Tang, Z. Xu, S. Yang et al., *Acoplanarity of QED pairs accompanied by nuclear dissociation in ultra-peripheral heavy ion collisions*, 2006.07365.
- [21] ATLAS collaboration, *Measurement of muon pairs produced via $\gamma\gamma$ scattering in nonultraperipheral Pb+Pb collisions at $\sqrt{s_{NN}} = 5.02$ TeV with the ATLAS detector*, *Phys. Rev. C* **107** (2023) 054907 [2206.12594].
- [22] PHENIX collaboration, *Low- p_T direct-photon production in Au+Au collisions at $\sqrt{s_{NN}} = 39$ and 62.4 GeV*, *Phys. Rev. C* **107** (2023) 024914 [2203.12354].
- [23] Z. Ye, “Thermal dileptons as a probe of extreme qcd matter created in heavy-ion collisions.” *Strangeness in Quark Matter (SQM) 2022 talk*, year = 2022, note = Accessed: 2023–21-06.
- [24] J.-H. Otto, “Virtual photon measurements with the hades at gsi.” *Quark Matter 2022 talk*, 2022.
- [25] CMS collaboration, *Observation of τ lepton pair production in ultraperipheral lead-lead collisions at $\sqrt{s_{NN}} = 5.02$ TeV*, 2206.05192.
- [26] ATLAS collaboration, *Observation of the $\gamma\gamma \rightarrow \tau\tau$ process in Pb+Pb collisions and constraints on the τ -lepton anomalous magnetic moment with the ATLAS detector*, 2204.13478.